Research Square

Preprints are preliminary reports that have not undergone peer review.
They should not be considered conclusive, used to inform clinical practice,
or referenced by the media as validated information.

Human placental extract regulates polarization of macrophages via IRGM/NLRP3 in allergic rhinitis

Xiaoming Li (xmlmo@126.com)
The 980th Hospital of the People's Liberation Army Joint Logistics Support Force
beibei Wo
The 980th Hospital of the People's Liberation Army Joint Logistics Support Force
chunyang du
Hebei Medical University
yan yang
Hebei Medical University
huimin qi
Hebei Medical University
zihui liang
Hebei Medical University
conghui he
The 980th Hospital of the People's Liberation Army Joint Logistics Support Force
fang yao
Hebei Medical University

Research Article

Keywords: Allergic rhinitis, Nod-like receptor protein 3 (NLRP3), Immunity-related GTPase M (IRGM), Human placenta extract (HPE), Macrophages polarization

Posted Date: December 29th, 2022

DOI: https://doi.org/10.21203/rs.3.rs-2394154/v1

License: This work is licensed under a Creative Commons Attribution 4.0 International License.
Read Full License

Abstract

Background: Allergic rhinitis (AR) is globally prevalent and its pathogenesis remains unclear. Alternative activation of macrophages is suggested in AR and thought to be involved in natural immunoregulatory processes in AR. Aberrant activation of Nod-like receptor protein 3 (NLRP3) inflammasome is linked with AR. Human placenta extract (HPE) is widely used in clinics due to its multiple therapeutic potential carried by diverse bioactive molecules. We aim to investigate the effect of HPE on AR and the possible underlying mechanism.

Methods: Ovalbumin (OVA)-induced AR rat model was set up and treated by HPE or cetirizine. General manifestation of AR was evaluated along with the histological and biochemical analysis performed on rat nasal mucosa. A proteomic analysis was performed on AR rat mucosa. Mouse alveolar macrophages (MH-S cells) were cultured under OVA stimulation to investigate the regulation of macrophages polarization. The morphological changes of nasal mucosa, the expression of NLRP3 inflammasome and immunity-related GTPase M (IRGM) in nasal mucosa as well as in MH-S cells were evaluated respectively.

Results: The general manifestation of AR along with the histological changes in nasal mucosa of AR rats were improved by HPE. HPE treatment suppressed NLRP3 inflammasome and the decline of IRGM in AR rats and MH-S cells. HPE regulates macrophage polarization through IRGM/ NLRP3 in AR.

Conclusions: HPE had protection for AR and the protection is achieved partly through suppressing M1 while promoting M2, the process which is mediated by IRGM via inhibiting NLRP3 inflammasome in AR

Background

Allergic rhinitis (AR) is a common disorder involving nasal mucosa. The classic symptoms, which are often triggered by airborne pollens, molds, dust mites and animal dander, include sneezing, rhinorrhea, nasal obstruction and nasal itching [1]. Epidemiologic studies suggest that 20 to 30% of adults and up to 40% of children are affected by AR and incur not only poor quality of life but heavy societal burden [2]. Though the pathogenesis of AR remains unclear, it is generally considered that the predominant process in this allergic inflammation is IgE-mediated immune responses to environmental allergen exposure [3]. Multiple inflammatory cells, such as B and T cells, eosinophils, basophils and mast cells, are involved in this inflammatory process [4]. Macrophages, as the important constituent of innate and adaptive immunity, act not only as antigen-presenting cells but have been thought to be involved in the regulation of the allergic immune responses by virtue of their ability to produce cytokines and inflammatory mediators [5, 6]. It is well recognized through large amounts of researches that macrophages are heterogeneous and the delicate balance between the polarization of M1 and M2 are critical to the fate of an organ in inflammation or injury [7]. Recently the alternative activation program in macrophages is also implied in AR and the study suggested M2 macrophages may play an important role in natural immunoregulatory processes in AR [8].

Nod-like receptor protein 3 (NLRP3) inflammasome, a key component of a multiprotein complex, belongs to the Nod-like receptors (NLRs) family and can be activated by diverse stimuli, e.g. RNA viruses, endogenous danger signals and environmental irritants[9]. The assembly and activation of NLRP3 inflammasome complex results in the activation of caspase-1, which subsequently activate the precursors of the inflammatory cytokines IL-1β and IL-18 [9]. It has been implicated that the activated NLRP3, along with the increased caspase-1, IL-1β and IL-18 either in patients or mice with AR, promotes the progression of AR, however suppression of NLRP3 ameliorates the nasal inflammation in AR mice models [10, 11]. Recently macrophages have been suggested to be involved in this contribution of NLRP3 to the development of AR via NLRP3-mediated pyroptosis [6]. Nevertheless the underlying mechanism of the role of macrophages in AR is far from being elucidated and the relationship between NLRP3 and polarization in macrophages need to be investigated.

Human placenta extract (HPE), prepared from the placenta of healthy pregnant females, is known to have diverse bioactive molecules with therapeutic potential for multiple uses including fatigue relief, skin whitening, wound healing and Anti-Aging [12–14]. HPE was also reported to have anti-stress effects, improve liver regeneration and reduce inflammation as well [15–17]. However, the effect of HPE on AR remains to be explored. Therefore, in the present study, we set up an ovalbumin (OVA)-induced AR rat model and evaluated the effects of HPE on AR. To investigate the underlying mechanism of the allergic inflammation in AR, a proteomics analysis as well as macrophages experiments in vitro were performed to reveal the possible regulation of polarization in macrophages.

Materials And Methods

Antibodies and other reagents

HPE used in the present experiments was commercially obtained from Handan Kangye Pharmaceutical Co. Ltd (Handan, Hebei, China). OVA was obtained from Sigma Chemical Co. (St. Louis, MO, USA). Antibodies against IRGM (GTX85038), IL-6 (GTX110527), and caspase 1 p10 (GTX134551) were purchased from GeneTex (Alton Pkwy Irvine, CA, USA). Antibodies against NLRP3 (ab263899), interleukin (IL)-1β (ab254360), IL-18 (ab191860) and β-actin (ab8226) were purchased from Abcam (Cambridge, UK). Antibodies for TNF-α (60291-1-Ig), IL-10 (60269-1-Ig), Arg-1 (16001-1-AP), and CD206 (18704-1-AP) was purchased from Proteintech (Chicago, IL, USA). Antibody for ASC (67824) was from Cell Signaling Technology (Beverly, MS). The goat anti-rabbit or mouse IgG-HRP secondary antibody was purchased from Zhongshan Golden bridge Biotechnology (Beijing, China). Alexa Fluor® 647 Rat Anti-Mouse CD206 (56525,),PE Rat Anti-Mouse F4/80 (565410), and FITC Rat Anti-Mouse CD86 (561962) were purchased from BD PharmingenTM. IRGM siRNA (sc-41794) was from Santa Cruz Biotechnology (Santa Cruz, CA, USA). NLRP3 siRNA was obtained from Gene Pharma Biotechnology (Shanghai, China). FuGENE-HD transfection reagent was obtained from Promega (Madison, WI, USA). Hematoxylin-Eosin (H&E), Giemsa and Alcian blue-Periodic acid Sciff (AB-PAS) staining kits were bought from Solarbio (Beijing, China), while Takara (Shiga, Japan) was the source of SYBR Premix Ex Taq II. The IRGM, IL-4, IL-5, IL-12, IL-13,

SIgE and Histamine enzyme-linked immunosorbent assay (ELISA) kits were purchased from Mbbiology Biological Technology Co., Ltd. (Yancheng, Jiangsu, China). All culture media and fetal bovine serum (FBS) were obtained from Gibco-BRL (Grand Island, NY, USA).

Animal model

Thirty male Sprague-Dawley (SD) rats (body weight: 200–220 g) were obtained from Weitonglihua Company (Beijing, China) and housed in a level specific pathogen free (SPF) animal room at room temperature 22–24°C with free access to water and food. The experiments and all the protocols were approved by the Ethics Review Committee for Animal Experimentation of Hebei Medical University (IACUC-Hebmu-PD-2021016). After a week of acclimation period, the rats were randomly divided into five experimental groups (n = 6): control group (Control), AR model group (AR), HPE treatment group (AR + HPE), solvent control group (AR + V) and cetirizine treatment group (AR + C). AR model rats were sensitized using OVA as follows. Ovalbumin (0.3mg) diluted in 1 ml sterile saline was administered along with $Al(OH)_3$ (30mg) to unanesthetized animals seven times by intraperitoneal (i.p.) injections on day 1, 3, 5, 7, 9, 11 and 13. Daily intranasal instillation with 50 mg/ml OVA (diluted with sterile saline, 20 μL per rat) were subjected from days 15 to 17, then instillation with 100mg/ml OVA from days 18 to 21. The control group were treated with the same volume of sterile saline and $Al(OH)_3$ without OVA with the same protocol instead. Once OVA-induced allergic rhinitis model established, the following treatments were performed on rats every 2 days in each group from days 28 to 46: rats in AR + HPE group or AR + V group were intraperitoneally injectied with HPE solution (4ml/5ml/kg) or vehicle (phenol solution made with saline, 2mg/5ml/kg) respectively; and rats in AR + C group were intragastrically administered with 5mg/5ml/kg cetirizine. The experimental process of AR mouse model is depicted in Fig. 1A. At the end of the experiment, the rats were anesthetized with sodium pentobarbital (150mg/kg, i.p.) and the blood of rats were collected before euthanasia. The nasal mucosal tissues of rats were also collected after sacrifice.

Behavioral assessment

24 hours after the last OVA administration (day 46), the frequency of nose-rubbing, the degree of runny nose, and the number of sneezes within 30 min were recorded. A scoring system was set up as follow to evaluate the symptoms of rhinitis. Nose-rubbing: 1–4 times, 1 point, > 4 times, 4 points; Runny nose: flow to the anterior nostrils, 1 point, over the front nostrils, 2 points, over the face, 3 points; Sneezing: 1–3 sneezes, 1 point; 4–10 sneezes, 2 points; >11 sneezes, 3 points. The rat with the total score over 5 points was regarded as the successful AR model.

Histological analysis of nasal mucosa

Nasal mucosa specimens were fixed in 10% neutral-buffered formalin overnight and then subject to alcohol and xylene dehydration respectively. Dehydrated specimens were immersed in paraffin and cut into 4-μm-thick sections. The sections were then dewaxed and stained with hematoxylin and eosin (H&E), Alcian Blue and Periodic acid-Schiff (AB-PAS) or Giemsa staining according to the manufacturer's

instructions. The final stained sections were photographed under a light microscope (BX-50 Olympus) at 200× magnification.

Immunofluorescence assays

The immunofluorescence samples were incubated with anti-TNF-α (1:600), anti-CD206 (1:1000), CD68 (1:1000) and IRGM (1:400) at 4°C overnight, and cell nuclei were counterstained with 4’6-diamidino-2-phenylindole (DAPI). The stained samples were imaged using an Olympus microscope (Olympus Corporation, Tokyo, Japan).

LC-MS/MS analysis and differentially expressed protein quantification

Liquid chromatography with tandem mass spectrometry (LC-MS/MS) analysis was performed at PTM BIO (PTM Biolabs, Hangzhou, Zhejiang, China). Briefly, nasal mucosa tissues were collected and digested. The tryptic peptides were cleaned with C18 ZipTips (Millipore) according to the manufacturer's instructions, followed by analysis with LC-MS/MS. The resulting MS/MS data were processed by using MaxQuant with integrated Andromeda search engine (version 1.5.2.8). False discovery rate thresholds for protein and peptide were specified at 1%. The subcellular localization prediction analysis of differentially expressed proteins was using Wolfpsort. The GO, domains, and Kyoto Encyclopedia of Genes and Genomes (KEGG) were used for functional enrichment analyses. A protein with a fold change > 1.5, and the presence of least 2 unique peptides with a P value < 0.05, was considered to be differentially expressed protein.

Cell culture and treatments

The mouse-derived alveolar macrophage cells, MH-S cell line was obtained from the National Infrastructure of Cell Line Resource (Being, China). Cells were cultured in DMEM supplemented with 10% fetal bovine serum, 100U/ml penicillin, 0.1mg/ml streptomycin at 37°C in a humidified incubator with 5% CO_2. MH-S cells were stimulated with different doses of OVA for 24 h to determine the best stimulation time and concentration. Cell viability were assessed with Cell Counting Kit-8 (CCK-8, HY-K0301, MedChemExpress, USA). MH-S cells were divided into five groups: cells in the control group were maintained with DMEM;cells in the OVA group were incubated with 10 μg/ml ovalbumin (OVA) for 24h cells in HPE treatment group, HPE (10 μM) were added 1h before OVA stimulation cells in vector control group, the same of volume of phenol solution (0.4mg/ml) were added 1h before OVA stimulation, and for the cetirizine treatment group, 5mM cetirizine added 1h before OVA stimulation. In addition, to investigate the signaling pathway which may regulate the function of macrophages in AR, thus further to reveal the underlying mechanism of the protective effect of HEP on AR, MH-S cells were transfected with *Irgm* overexpression plasmid pcDNA3.1(+), IRGM siRNA or NLRP3 siRNA for 24h, and then treated with HPE (10 μM) for 1h before OVA stimulation. The siRNA duplexes used were: IRGM-siRNA-1, 5'-GGGCUGGGAUUCUGUCAUA-3'; IRGM-siRNA-2, 5'-GA GGTGATCTCTAACATCA – 3'; IRGM-siRNA-3, 5'-TGGCAATGGCATG TCATCTT-3'; NLRP3-siRNA, 5'-CATGAAGAGAACTTTCATGAGTG TC-3'; Scr-siRNA, 5'-CGUACGCGGAAUACUUCGAUU-3'. All cell experiments were repeated independently at least three times.

Enzyme-linked immunosorbent assay (ELISA)

Blood samples of each rat and the supernatants from different groups of MH-S cells were collected respectively. The levels of inflammatory cytokines (IL-4, IL-5, IL-12, IL-13), anti-OVA specific IgE and histamine were measured using commercially available ELISA kits according to the manufacturer's recommendations. The amount of cytokine was calculated from the equation obtained from a standard curve plot for each cytokine standard solution in the kit.

Protein extraction and Western blotting analysis

Cell lysate was extracted from nasal mucosa tissues and MH-S cells on ice with RIPA lysis buffer (Millipore, Billerica, MA, USA) according to the standard procedure. Equal amounts of total protein (30 μg/lane) were loaded and resolved by 10% sodium dodecyl-sulfate polyacrylamide gel electrophoresis (SDS-PAGE) and transferred onto polyvinylidene difluoride (PVDF) membranes (Millipore, Billerica, MA). After blocking with 5% skimmed milk, the membranes were incubated with primary antibodies (anti-NLRP3, IRGM, ASC, IL-1β, Caspase1 p10, TNF-α, CD206, IL-6, IL-10 and β-actin) overnight at 4°C. Image acquisition was performed using the chemiluminescent Amersham Imager 600, and band densitometry was performed using ImageJ software (NIH).

RNA isolation and quantitative real-time RT-PCR

Total RNA and then cDNA were prepared from nasal tissues and cultured MH-S cells using TRIzol reagent (Invitrogen, Carlsbad, CA) and Takara RNA PCR kit (AMV) Ver. 3.0 (Takara Bio Inc., Shiga, Japan). PCR primers (Table 1) were designed and synthesized by Sangon Biotech Co, Ltd. (Shanghai, China). Real-time PCR was performed using SYBR Premix Ex TaqTMII and reactions were performed on Agilent Mx3000P QPCR Systems (Agilent, CA). The levels of target mRNA were normalized to 18s rRNA and all experiments were repeated at least three times.

Table 1
The sequences of PCR primer pairs used in this study

Gene	Forward primers (5′-3′)	Reverse primers (5′-3′)
Rat-NLRP3	CCTGGGGGACT TTGGAATCAG	GATCCTG ACAACAC GCGGA
Rat-ASC	GTGGGTGGCTTTCCTT GATT	TTGTCTT GGCTGGTGGTC TCT
Rat-IL-1β	GCCCATCCTCTGTGAC TCAT	AGGCCACAGGTATTTTGTC
Rat-Caspase-1 p10	TTTCCGCAAGGTTC GATTTTCA	GGCATCTGCGCTCTAC CATC
Rat-ACSM3	AGGAAGATGCTACGTCATGCC	ATCCCCAGTTTGAAGTCCTGT
Rat-Tmed7	TTGGAGAAGACCCACCTTTG	GCCCTATGCTAACCACCAGA
Rat-IRGM	ATGACATACTCAGCACCGGC	AGTACTCAGTCCGCGTCTTCGT
Rat-Ighm	CATCCCTCCCTCCTTTGC	TCATAGGTGCCCAGGTTTG
Rat-Agt	CATCTTCCCTCGCTCTCTG	GCCTCTCATCTTCCCTTGG
Rat-Ank1	ATGTGGACCTTCATCA	AGGGGCAAGCAGTGA
Rat-Adh7	ACCCGAAGCGGACATT	GGCATCTCCCTGAACG
Rat-GAPDH	GGCAAGTTCAACGGCACAGT	ATGACATACTCAGCACCGGC
Mouse-NLRP3	ATTACCCGCCCGAGAAAGG	TCGCAGCAAAGATCCACACAG
Mouse-ASC	CTTGTCAGGGGATGAACTCAA	CTGGTCCACAAAGTGTCCTGT
Mouse-IL-1β	TGCCACCTTTTGACAGTGATG	TGTGCTGCTGCGAGATTTGA
Mouse-Caspase-1 p10	CACAGCTCTGGAGATGGTGA	CTTTCAAGCTTGGGCACTTC
Mouse-IL-6	AGACAAAGCCAGAGTCCTTCAGAGA	GCCACTCCTTCTGTGACTCCAGC
Mouse-TNF-α	ACGTGGAACTGGCAGAAGAG	CTCCTCCACTTGGTGGTTTG
Mouse-Arg-1	AGACAGCAGAGGAGGTGAAGAGTAC	GGTAGTCAGTCCCTGGCTTATGGT
Mouse-IL-10	CGACGCTGTCATCGATTTCTC	CAGTAGATGCCGGGTGGTTC
Mouse-18s	CGGCTACCACATCCAAGGAA	GCTGGAATTACCGCGGCT

Flow cytometry assays

At the end of cell experiments, MH-S cells were harvested and M1 and M2 as well as microphases marker were detected with flow cytometry (FACSCalibur, BD Biosciences) by detecting labeled FITC anti-CD86, Alexa Fluor® 647 anti-CD206 and PE anti-F4/80, The percentage of M1 or M2 was analyzed using FlowJo 10 software (FlowJo LLC).

Statistical analysis

The results from at least three independent experiments are expressed as the mean ± standard error of the mean. Statistical analysis of the data was performed with one-way analysis of variance (ANOVA) followed by a Dunnett's test for multiple comparisons. GraphPad Prism 5.01 (GraphPad Software Inc.) was used for data analysis and statistical significance was set at $P < 0.05$.

Results

HPE improves the general manifestation of AR

1. HPE relieves the symptoms of AR

AR rat model was successfully established according to the symptom scoring methods described before. The number of sneezes and nose-rubbing events within 30 min were significantly increased in OVA-induced rats (AR rats) compared to control, while AR rats treated with HPE or cetirizine showed much less sneezes or nose rubbing than AR rats (Fig. 1B and C). The frequency of AR symptoms in vector only-treated AR rats is similar to that in AR rats (Fig. 1B and C). No significant differences were found between HPE and cetirizine treatment group (Fig. 1B and C). These results demonstrated that HPE administration significantly relieved the symptoms of AR in rats.

2. HPE decreases serum proinflammatory cytokine levels in AR

To assess the degree of AR-associated inflammation, the serum levels of several inflammatory cytokines were determined by ELISA. The levels of Th2 cytokines, IL-4, IL-5 and IL-13, were significantly increased in AR rats compared with those in control group (Fig. 1D-F). Administration of HPE or cetirizine significantly decreased the IL-4 and IL-13 levels, but the effect on IL-5 did not reach significance (Fig. 1D-F). Conversely, the level of IL-12, a Th1 cytokine, markedly dropped in AR rats comparing to control rats, whereas HPE or cetirizine treatment substantially reverse this decline in rats with AR (Fig. 1G). Furthermore, HPE or cetirizine treatment showed obvious suppression on the levels of OVA-induced IgE and histamine in AR rats (Fig. 1H and I). The efficacy between HPE and cetirizine showed no significant difference and the vector treatment showed no significant effects on AR rats (Fig. 1).

HPE improves the histological changes of the nasal mucosa in AR rats

The effects of HPE on the histological changes in nasal mucosa was evaluated by HE, Giemsa, AB-PAS and Masson trichrome staining. H&E and Giemsa staining showed the nasal mucosa of rats in the control group were in normal state as the lining epithelia kept intact without inflammatory cell infiltration (Fig. 2A). By contrast, broken and exfoliated epithelia with plenty of eosinophils and mast cells infiltration were observed in the nasal mucosa of AR rats (Fig. 2A-C). HPE or cetirizine treatment greatly improved

the changes of nasal mucosa from the AR rats with much less eosinophils and mast cells infiltration than those from none or vector only-treated AR rats (Fig. 2A-C).

Goblet cells in nasal mucosa of rats were visualized by AB-PAS staining, which showed the characteristic mucin in goblet cells as turquoise vesicles (Fig. 2A). A great many of large mucinous vesicles in AR group confirmed the prominent hypertrophy and proliferation of goblet cells in the nasal mucosa in AR (Fig. 2A). HPE or cetirizine treatment greatly reduced both the number and the size of goblet cells in AR rats (Fig. 2A and D). In addition, Masson staining was performed to assess the distribution of extracellular matrix (ECM) in the nasal mucosa, and the results showed enhanced ECM deposition, presenting as more and darker blue areas in nasal mucosa of AR rats compared to control group (Fig. 2A and E). Apparently, HPE or cetirizine treatment effectively prevented collagen deposition in AR rats (Fig. 2A and E). Neither the comparison between HPE-treated and cetirizine-treated groups nor that of between AR rats without and with only vector treatment showed significant differences (Fig. 2).

HPE suppresses NLRP3 inflammasome in AR rats

The mRNA and protein expression of NLRP3, apoptosis associated speck like protein containing a CARD (ASC), caspase-1 p10 and cleaved IL-1β, were detected in the nasal mucosa of rats to assess the activation of NLRP3 inflammasome. The results of western blot revealed that the protein levels of NLRP3, ASC, caspase-1 p10 and cleaved IL-1β were increased in AR rats compared with those in control rats, and HPE or cetirizine treatment drastically attenuated these increases in rats with AR (Fig. 3A-C). Furthermore, the mRNA expression levels of NLRP3 and ASC in AR group exhibited significant upregulation while these changes were greatly reversed in HPE or cetirizine-treated group (Fig. 3D and E). Moreover, this markedly increased NLRP3 protein expression was also detected by IHC staining in nasal mucosa of AR rats compared to control (Fig. 3F and G). Being consistent with the results of western blot and real-time RT-PCR, the results of IHC in HEP or cetirizine-treated rats reconfirmed the suppressing effect of HEP or cetirizine on NLRP3 inflammasome (Fig. 3F and G) and no significant differences showed between these two groups (Fig. 3).

HPE suppresses the decline of IRGM in AR rats

To clarify the underlying mechanism of HPE's anti-inflammation effects, nasal mucosa tissues from rats in control, AR and HPE-treated AR groups were subjected to high-resolution LC-MS/MS to perform proteomics analysis. 53 distinct proteins were screened out between control and AR rats, including 22 downregulated proteins and 31 up-regulated proteins (Fig. 4A). In addition, 257 distinct proteins were found between HPE-treated AR rats and AR rats, including 105 downregulated proteins and 152 up-regulated proteins ($\geq$ 2-fold change in expression level; $P < 0.05$) (Fig. 4A). Gene ontology (GO) and Kyoto Encyclopedia of Genes and Genomes (KEGG) pathway analysis revealed that differentially expressed proteins of nasal mucosa in HPE-treated rats were strongly associated with regulation of inflammatory response, extracellular matrix organization, and immune system process (Fig. 4B and C).

Subsequently, 7 differentially expressed factors with significant changes in HPE-treated group were verified by qRT-PCR. The consequence showed the mRNA level of immunity-related GTPase M (IRGM)

was the most changed and downregulated in AR rats but dramatically most reversed by HPE treatment (Fig. 4D). Meanwhile the protein expression of IRGM and its serum levels were detected by western blot and ELSIA respectively. The consequences showed the changes of IRGM either on protein level or in serum were consistent with the changes of its mRNA (Fig. 4E-G). Double immunofluorescence staining presented the colocalization of IRGM with CD68, which suggested IRGM was within macrophages (Fig. 4H). The results of the double staining further confirm the dramatic decreases of IRGM in nasal mucosa of AR rats and these decreases were markedly reversed by HPE or cetirizine treatment in rats with AR (Fig. 4H and I). However interestingly, we found the changes of IRGM was not parallel to the changes of macrophage counts as the interstitial macrophages infiltration in nasal mucosa increased in all AR groups including the rats with or without any treatment while more colocalization of CD68 and IRGM presented in nasal mucosa in HPE or cetirizine-treated group (Fig. 4H and I).

HPE regulates macrophage polarization through IRGM/NLRP3

Enlightened by the unparalleled changes of IRGM within infiltrating macrophages, we further interrogated whether different subtypes of macrophages are involved and contribute differently to AR.

1. HPE regulates macrophage polarization in AR rats and MH-S cells

Double immunofluorescence staining showed much more colocalization of CD68 and TNF-α in nasal turbinate mucosa from AR rats than control, which implied macrophages were dramatically activated and polarized to M1 in AR (Fig. 5A and B). HPE or cetirizine treatment greatly reversed this activation and transition of macrophages in AR rats (Fig. 5A and B). Double staining of CD68 and CD206 showed M2 macrophages also increased in nasal mucosa of AR rats compared to control (Fig. 5A and C). However, in contrast to the suppression effects on M1 polarization, HPE or cetirizine treatment drastically enhanced M2 polarization in AR rats (Fig. 5A and C). To clarify the regulation of macrophages polarization in AR, mouse alveolar macrophage cells (MH-S cells) were cultured and stimulated with OVA at different concentration. OVA with the concentration 40μm/L was determined as the stimulus in cell culture experiments according to cell viability assessment (Fig. 5D). IL-6 and TNF-α, the representative inflammatory cytokines of M1 as well as Arginase-1 (Arg-1) and IL-10, the representative cytokines of M2 were detected at mRNA and protein level respectively. qRT-PCR results indicated that both M1 and M2 cytokines in MH-S cells were induced by OVA stimulation, but the levels of IL-6 and TNF-α in MH-S cells rise more prominently than Arg-1 and IL-10 (Fig. 5E and F). HPE or cetirizine treatment before OVA stimulation markedly suppressed the induction of M1 while promoted the M2 cytokines to greater levels (Fig. 5E and F). The results of western blot experiments showed the changes of protein expressions of M1 and M2 cytokines were proximately consistent with those of mRNA levels of M1 and M2 cytokines (Fig. 5G-I). The above results of MH-S polarization were verified by flow cytometry assay. MH-S cells were sorted as non-activated macrophages, M1 and M2 by gating cells with F4/80, CD86 and CD206 (Fig. 5J). Flow cytometry analysis showed, comparing with control, OVA stimulation activated MH-S cells with

more M1(13.8% vs 0.037%) and M2 (7.21% vs 0.13%). Comparing with OVA group, HPE or cetirizine treatment significantly promoted M2 (36.4% or 21.2% vs 7.21%) while greatly suppressed M1 (0.13% or 0.7% vs 13.8%) (Fig. 5, J and K). No significant differences were detected between OVA group and vector control groups (Fig. 5).

2. HPE regulates OVA-induced polarization of MH-S cells by upregulating IRGM

IRGM protein in MH-S cells were significantly decreased by OVA (40μm/L or 50μm/L) simulation at 24h (Fig. 6A and B). The results of time-course experiment showed the expression of IRGM in MH-S cells under the stimulation of OVA (40μm/L) decreased from 4h and was down to about 20% of its original expression at 24h (Fig. 6C and D). HPE or cetirizine treatment reversed the suppression of IRGM induced by OVA (Fig. 6E and F). To investigate the role that IRGM played in macrophages polarization, MH-S cells were transfected with IRGM siRNA or overexpression plasmid. IRGM siRNA 2 was picked from 3 designed siRNA for its most prominent knockdown effect on IRGM protein (Fig. 6G and H). The efficacy of IRGM overexpression plasmid was also verified by western blot (Fig. 6I and J). The results of qRT-PCR and western blot showed IL-6 and TNF-α in MH-S cells were markedly increased by OVA stimulation while Arg-1 and IL-10 were less prominent though also increased in MH-S cells, which implied that MH-S skewed to M1 predominance by the induction of OVA (Fig. 6K-M). IRGM overexpression or HPE treatment reversed this skew and promoted greater proportion of MH-S cells to M2 while conversely IRGM knockdown almost abrogated the effects of HPE on MH-S skew correction (Fig. 6K-M).

3. IRGM regulates MH-S cells polarization via suppressing NLRP3 inflammasome

OVA stimulation resulted in upregulation of NLRP3 inflammasome (NLRP3, ASC) with the activation of its downstream pro-inflammatory cytokine IL-1β (cleaved IL-1β) and caspase 1 (caspase-1 p10) in MH-S cells (Fig. 7A and B). MH-S cells immunofluorescence staining further confirmed the upregulation of NLRP3 induced by OVA stimulation (Fig. 7C and D). The results of Western blot and immunofluorescence staining suggested HPE treatment or IRGM overexpression greatly suppressed OVA-induced upregulation and activation of NLRP3 inflammasome while IRGM silencing before HPE treatment abrogated the suppression effect of HPE on NLRP3 inflammasome (Fig. 7A-D).

To investigate whether NLRP3 inflammasome regulates macrophages polarization, NLRP3 siRNA was transfected into MH-S cells. The efficacy of NLRP3 siRNA was verified through downregulation and deactivation of NLRP3 inflammasome (Fig. 7E and F). qRT-PCR and western blot showed, like the HPE treatment working on MH-S cell polarization, NLRP3 knockdown markedly suppressed the OVA-induced expression of IL-6 and TNF-α while enhanced the expression of Arg-1 and IL-10 to greater levels, which implies NLRP3 mediates OVA-induced M1 skew in MH-S cells (Fig. 7G-J). All results from vector control groups were not significantly different from OVA groups (Fig. 7).

Discussion

Evidences extrapolated from clinical and lab researches suggest AR-associated inflammation is primarily T helper (Th) 2 cell-driven inflammation [3]. Briefly, antigen presenting cells including dendritic cells and macrophages present processed allergen to naive T cells and the latter are subsequently polarized into effector memory allergen specific Th2 cells, which by releasing IL-4, IL-5, IL-9 and IL-13 promote Ig E production in B lymphocytes as well as attract and recruit mast cell, basophils and eosinophils. On allergen re-exposure, crosslinking complexes of sensitized IgE with FcεRI at the surface of mast cells and basophils lead to degranulation and the release of mediators such as histamine, tryptase and arachidonic acid derivatives [18–20]. In the present study, OVA-induced AR rat model was established with typical AR symptoms and morphological changes as well as increased serous Th2 cell cytokines. In addition to general histological changes such as damaged nasal epithelium with infiltration of mast cell and eosinophils in AR, goblet cell proliferation and enhanced ECM deposition were observed in nasal mucosa. Unlike the consensus on the characteristic tissue remodeling in asthma, this upper airway remodeling issue in AR remains controversial [21, 22]. Corren et al. suggest methodological differences including histologic assessment, subject grouping as well as differences in employed assays may partly explain this inconsistency of results across studies [23, 24]. In our study we administered cetirizine, a H1 antihistamine, as positive control of treatment to AR rats, to assess the effect of HPE on AR. According to the results, HPE exhibited remarkable antiallergic potency comparable to cetirizine either in respect of relief of AR symptoms or in suppression of Th2 cell cytokines. Moreover HPE, like cetirizine did in AR rats, also partially reversed the histological changes including some remodeling manifestation of AR. It was reported topical decongestant being significantly less effective on nasal obstruction in some patients with longer duration of rhinitis, which the researchers thought may be partly attributed to remodeling of the nasal mucosa [24]. Considering OVA-induced AR model applied in this study was acute AR, whether the anti-remodeling effects of HPE or cetirizine pertain to chronic AR need long-term observation.

In the present study, in addition to infiltration of mast cells and eosinophils in nasal mucosa in AR rats, enhanced macrophage infiltration was also founded in AR rats' nasal mucosa, which implied macrophages had been involved allergic inflammation in AR. However, this increase of macrophages did not decline as the former two cells did with the mitigation of AR symptoms after the treatment with HPE or cetirizine. The anti-allergic effects of HPE or cetirizine on AR seemed not to be achieved through changing the number of macrophages in nasal mucosa. To investigate the pathogenesis of AR and the underlying mechanisms of HPE's antiallergic effects on AR, proteomic analysis was applied and IRGM was screened out as the most changed (downregulated) cytokine in AR, meanwhile the most reversed by HPE treatment. What we found particularly intriguing in the subsequent colocalization assay with double immunofluorescence staining was that HPE or cetirizine treatment led to more IRGM-laden macrophages in nasal mucosa while didn't change the infiltration degree of macrophages in AR rats. Enlightened by this consequence, we hypothesized different subtypes of macrophages with different functions might be involved in AR and IRGM might be related to the differentiation of macrophages in AR. Further double immunofluorescence staining assay verified that the predominant infiltrating macrophages in AR rats' nasal mucosa were M1(TNF-a^+/$CD68^+$) whereas HPE or cetirizine treatment resulted in a higher proportion of M2 ($CD206^+$/$CD68^+$) among infiltrating macrophages in nasal turbinate mucosa of AR rats.

This results partly explain the HPE protective effect on AR for HPE suppressing pro-inflammatory macrophages M1 while promoting anti-inflammatory type of macrophages M2 in nasal mucosa.

IRGM has been associated with a variety of inflammatory diseases including tuberculosis, autoimmune thyroiditis, and ankylosing spondylitis since a genome-wide association study linked several SNPs near the IRGM locus to Crohn's disease [25, 26]. To clarify whether IRGM regulated macrophages polarization in AR, a mouse alveolar macrophage cell line, MH-S cells was introduced in this study. We found OVA stimulation, the sensitizer we used in this study to set up AR model, skewed MH-S cells to M1 while overexpression of IRGM corrected this skew and promoted MH-S cells to M2 predominance, which we found was similar to the effect that HPE or cetirizine treatment had on MH-S cells under the same OVA stimulation. Conversely, depletion of IRGM in MH-S cells abrogated the effect of HPE or cetirizine on MH-S cells polarization. Moreover, both IRGM overexpression and HPE or cetirizine treatment restrained OVA-induced upregulation and activation of NLRP3 inflammasome in MH-S cells. Aberrant activation of NLRP3 inflammasome has been linked with several inflammatory disorders including AR [27, 28]. Our study also detected activated NLRP3 inflammasome in nasal mucosa of AR rats. Along with the regulating effects of HPE or cetirizine on macrophages polarization in nasal mucosa, NLRP3 inflammasome is markedly suppressed and deactivated by HPE or cetirizine treatment in AR rats. Considering HPE treatment suppressing the IRGM decline in either AR rats or OVA-stimulated MH-S cells meanwhile IRGM overexpression deactivating NLRP3 inflammasome in MH-S cells, we supposed that the effect of HPE on macrophages polarization in AR might be mediated by IRGM through regulating NLRP3 inflammasome. The results from NLRP3 silencing experiments verified our hypothesis. Like IRGM changed the polarization of MH-S cells, depletion of NLRP3 could also correct the M1 skew and promote M2 differentiation among MH-S cells, which implied IRGM regulating macrophages polarization through inhibiting NLRP3 inflammasome. The underlying mechanism that IRGM inhibiting NLRP3 inflammasome was suggested to be related to NLRP3 inflammasome assembly and autophagy [29, 30]. IRGM was suggested in early functional studies as a positive regulator of autophagy [29]. Mehto et al. demonstrated IRGM inhibiting NLRP3 inflammasome by inhibiting its oligomerization and selective autophagic degradation of NLRP3 and ASC [30]. Although the mechanism underlying the regulation of macrophages polarization by NLRP3 inhibition need to be dug, the results of our study demonstrate that IRGM regulates macrophages polarization in AR through inhibiting NLRP3 inflammasome. HPE protective effect on AR is partly attributed to its regulation of macrophages polarization in nasal mucosa.

Conclusions

HPE has protection for AR and the protection is achieved partly through suppressing M1 while promoting M2, the process which is mediated by IRGM via inhibiting NLRP3 inflammasome in AR (Fig. 8). Our findings provide insight into the pathogenesis of AR and highlight the promising therapeutic strategies targeting IRGM-NLRP3 for AR in future.

Abbreviations

AR Allergic rhinitis

HPE Human placenta extract

NLRP3 Nod-like receptor protein 3

OVA Ovalbumin

IRGM immunity-related GTPase M

SD Sprague-Dawley

SPF specific pathogen free

HE Hematoxylin–eosin

AB-PAS Alcian Blue and Periodic acid-Schiff

ELISA Enzyme-linked immunosorbent assay

IL Interleukin

TNF Tumor necrosis factor

PVDF polyvinylidene difluoride

Declarations

Acknowledgments

Not applicable.

Author contributions

BBW and XML conceived and designed the project. FY, YY, HMQ, ZHL and CHH were in charge of literature investigation and experiment performance. CYD and BBW contributed to data analysis and interpretation of the results. CYD and FY wrote the original manuscript. BBW and XML assisted in revising the manuscript. All authors reviewed and approved the final manuscript.

Funding

This study was supported by grants from the Natural Science Foundation of Hebei province (No. H2020206340), Major project of Hebei Health Commission (No. 20201336), Youth Foundation of Hebei Education Department (No. QN2021104).

Availability of data and materials

The authors hereby declare that the data and materials in this study will be presented upon request from the corresponding author.

Ethics approval and consent to participate

The study was approved by the Ethics Review Committee for Animal Experimentation of Hebei Medical University (IACUC-Hebmu-PD-2021016).

Consent for publishlication

We declare that the Publisher has the authors' permission to publish the relevant contribution.

Competing interests

The authors declare no competing interest.

Footnotes

Publisher's Note

Springer Nature remains neutral with regard to jurisdictional claims in published maps and institutional affiliations.

Beibei Wo and Chunyang Du made equal contribution to the work.

Contributor Information

Xiaoming Li, Email: xmlmo@126.com.

Fang Yao, E-mail: yaofang2006@hotmail.com.

References

1. Schuler Iv CF, Montejo JM. Allergic Rhinitis in Children and Adolescents. Pediatr Clin North Am. 2019;66:981–93.
2. Meltzer EO. Allergic Rhinitis: Burden of Illness, Quality of Life, Comorbidities, and Control. Immunol Allergy Clin North Am. 2016;36:235–48.
3. Eifan AO, Durham SR. Pathogenesis of rhinitis. Clin Exp Allergy. 2016;46:1139–51.
4. Zhang S, Lin S, Tang Q, Yan Z. Knockdown of miR2055p alleviates the inflammatory response in allergic rhinitis by targeting Bcell lymphoma 6. Mol Med Rep. 2021;24:818.
5. Saradna A, Do DC, Kumar S, Fu QL, Gao P. Macrophage polarization and allergic asthma. Transl Res. 2018;191:1–14.

6. Zhou H, Zhang W, Qin D, et al. Activation of NLRP3 inflammasome contributes to the inflammatory response to allergic rhinitis via macrophage pyroptosis. Int Immunopharmacol. 2022;110:109012.
7. Shapouri-Moghaddam A, Mohammadian S, Vazini H, et al. Macrophage plasticity, polarization, and function in health and disease. J Cell Physiol. 2018;233:6425–40.
8. Lou H, Huang Y, Chen H, Wang Y, Zhang L, Wang C. M2 macrophages correlated with symptom severity and promote type 2 inflammation in allergic rhinitis. Allergy. 2019;74:2255–7.
9. Xiao Y, Xu W, Su W. NLRP3 inflammasome: A likely target for the treatment of allergic diseases. Clin Exp Allergy. 2018;48:1080–91.
10. Yang Z, Liang C, Wang T, et al. NLRP3 inflammasome activation promotes the development of allergic rhinitis via epithelium pyroptosis. Biochem Biophys Res Commun. 2020;522:61–7.
11. Activation of NLRP3 inflammasomeXiao. Jiang L, Hu L, Li Q. Y. MicroRNA-133b Ameliorates Allergic Inflammation and Symptom in Murine Model of Allergic Rhinitis by Targeting Nlrp3. Cell Physiol Biochem 2017; 42:901–12.
12. De D, Chakraborty PD, Bhattacharyya D. Regulation of trypsin activity by peptide fraction of an aqueous extract of human placenta used as wound healer. J Cell Physiol. 2011;226:2033–40.
13. Hong JW, Lee WJ, Hahn SB, Kim BJ, Lew DH. The effect of human placenta extract in a wound healing model. Ann Plast Surg. 2010;65:96–100.
14. Kong M, Park SB. Effect of human placental extract on health status in elderly koreans. *Evid Based Complement Alternat Med.* 2012; **2012**:732915.
15. Park HJ, Shim HS, Lee S, et al. Anti-stress effects of human placenta extract: possible involvement of the oxidative stress system in rats. BMC Complement Altern Med. 2018;18:149.
16. Jung J, Moon JW, Choi JH, Lee YW, Park SH, Kim GJ. Epigenetic Alterations of IL-6/STAT3 Signaling by Placental Stem Cells Promote Hepatic Regeneration in a Rat Model with CCl4-induced Liver Injury. Int J Stem Cells. 2015;8:79–89.
17. Chatterjee P, Chiasson VL, Pinzur L, et al. Human placenta-derived stromal cells decrease inflammation, placental injury and blood pressure in hypertensive pregnant mice. Clin Sci. 2016;130:513–23.
18. Takano K, Kojima T, Go M, et al. HLA-DR- and CD11c-positive dendritic cells penetrate beyond well-developed epithelial tight junctions in human nasal mucosa of allergic rhinitis. J Histochem Cytochem. 2005;53:611–9.
19. Hammad H, Chieppa M, Perros F, Willart MA, Germain RN, Lambrecht BN. House dust mite allergen induces asthma via Toll-like receptor 4 triggering of airway structural cells. Nat Med. 2009;15:410–6.
20. Jahnsen FL, Gran E, Haye R, Brandtzaeg P. Human nasal mucosa contains antigen-presenting cells of strikingly different functional phenotypes. Am J Respir Cell Mol Biol. 2004;30:31–7.
21. Bousquet J, Jacot W, Vignola AM, Bachert C, Van Cauwenberge P. Allergic rhinitis: a disease remodeling the upper airways? J Allergy Clin Immunol. 2004;113:43–9.

22. Eifan AO, Orban NT, Jacobson MR, Durham SR. Severe Persistent Allergic Rhinitis. Inflammation but No Histologic Features of Structural Upper Airway Remodeling. Am J Respir Crit Care Med. 2015;192:1431–9.
23. Corren J, Togias A. Remodeling in Allergic Rhinitis. Adding New Data to an Old Debate. Am J Respir Crit Care Med. 2015;192:1403–4.
24. Ciprandi G, Klersy C, Ameli F, Cirillo I. Clinical assessment of a nasal decongestion test by visual analog scale in allergic rhinitis. Am J Rhinol. 2008;22:502–5.
25. Nabar NR, Kehrl JH. Inflammasome Inhibition Links IRGM to Innate Immunity. Mol Cell. 2019;73:391–2.
26. Wellcome Trust Case Control C. Genome-wide association study of 14,000 cases of seven common diseases and 3,000 shared controls. Nature. 2007;447:661–78.
27. Kelley N, Jeltema D, Duan Y, He Y. The NLRP3 Inflammasome: An Overview of Mechanisms of Activation and Regulation. Int J Mol Sci. 2019;20:3328.
28. Leszczynska K, Jakubczyk D, Gorska S. The NLRP3 inflammasome as a new target in respiratory disorders treatment. Front Immunol. 2022;13:1006654.
29. Singh SB, Davis AS, Taylor GA, Deretic V. Human IRGM induces autophagy to eliminate intracellular mycobacteria. Science. 2006;313:1438–41.
30. Mehto S, Jena KK, Nath P, et al. The Crohn's Disease Risk Factor IRGM Limits NLRP3 Inflammasome Activation by Impeding Its Assembly and by Mediating Its Selective Autophagy. Mol Cell. 2019;73:429–45.

Figures

Fig.1

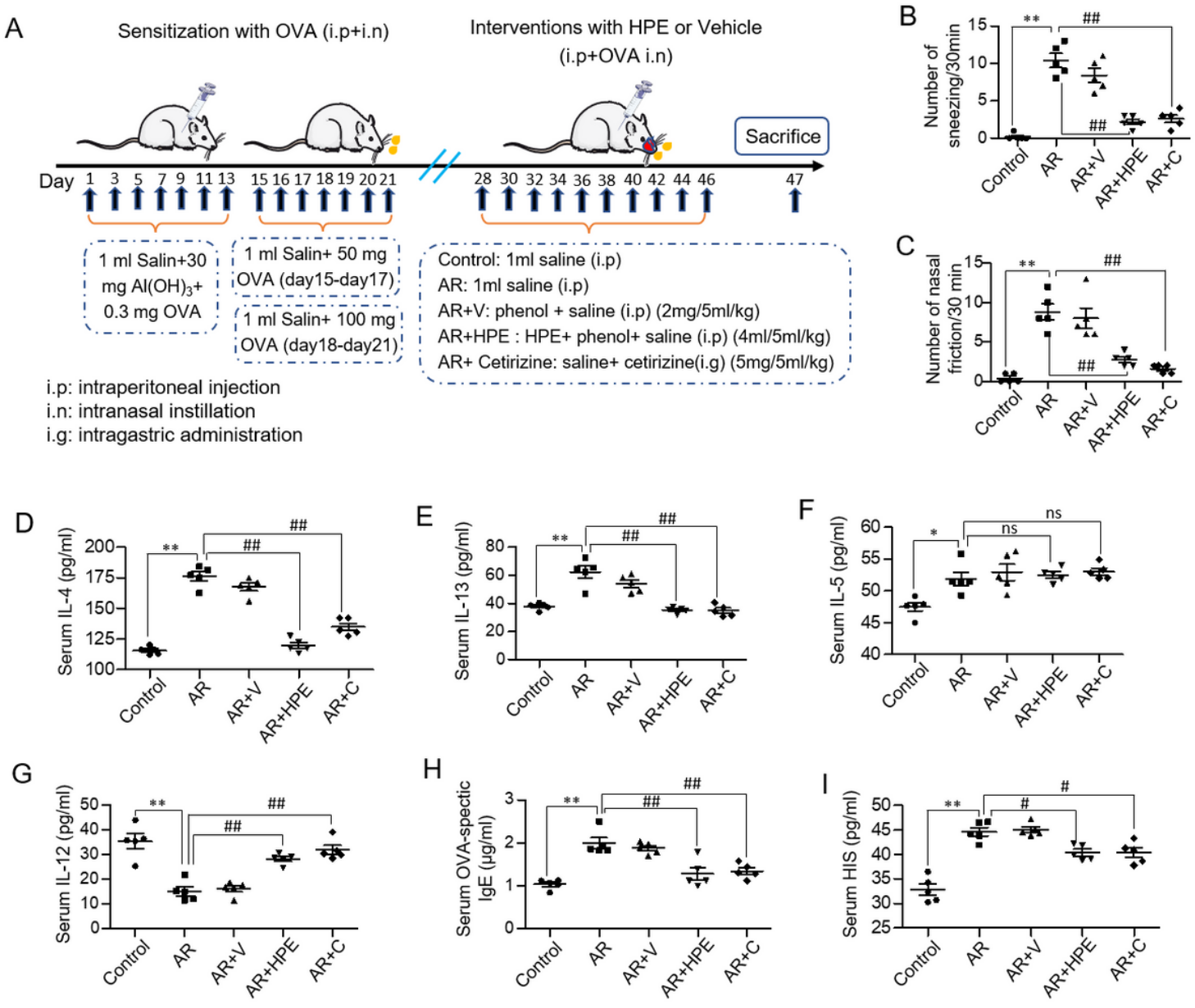

Figure 1

HPE improves the general manifestation of AR. (A) The experimental procedures for the rat model of AR. (B) The counts of sneezes within 30 min of each indicated group (n=5). (C) The counts of nose-rubbing events within 30 min in the indicated groups (n=5). D-I The measurements of inflammatory cytokines IL-4, IL-13, IL-5, IL-12, OVA-specific IgE and histamine in the serum of AR rats by ELISA (n=5). Values are expressed as means ± SEM. $^{*}p < 0.05$, $^{**}p < 0.01$ vs. Control group; $^{\#}p < 0.05$, $^{\#\#}p < 0.01$ vs. AR group. AR: allergic rhinitis; V: vehicle; HPE: human placenta extract; C: cetirizine; IL: interleukin; IgE: immunoglobulin E; HIS: histamine; OVA: ovalbumin.

Fig.2

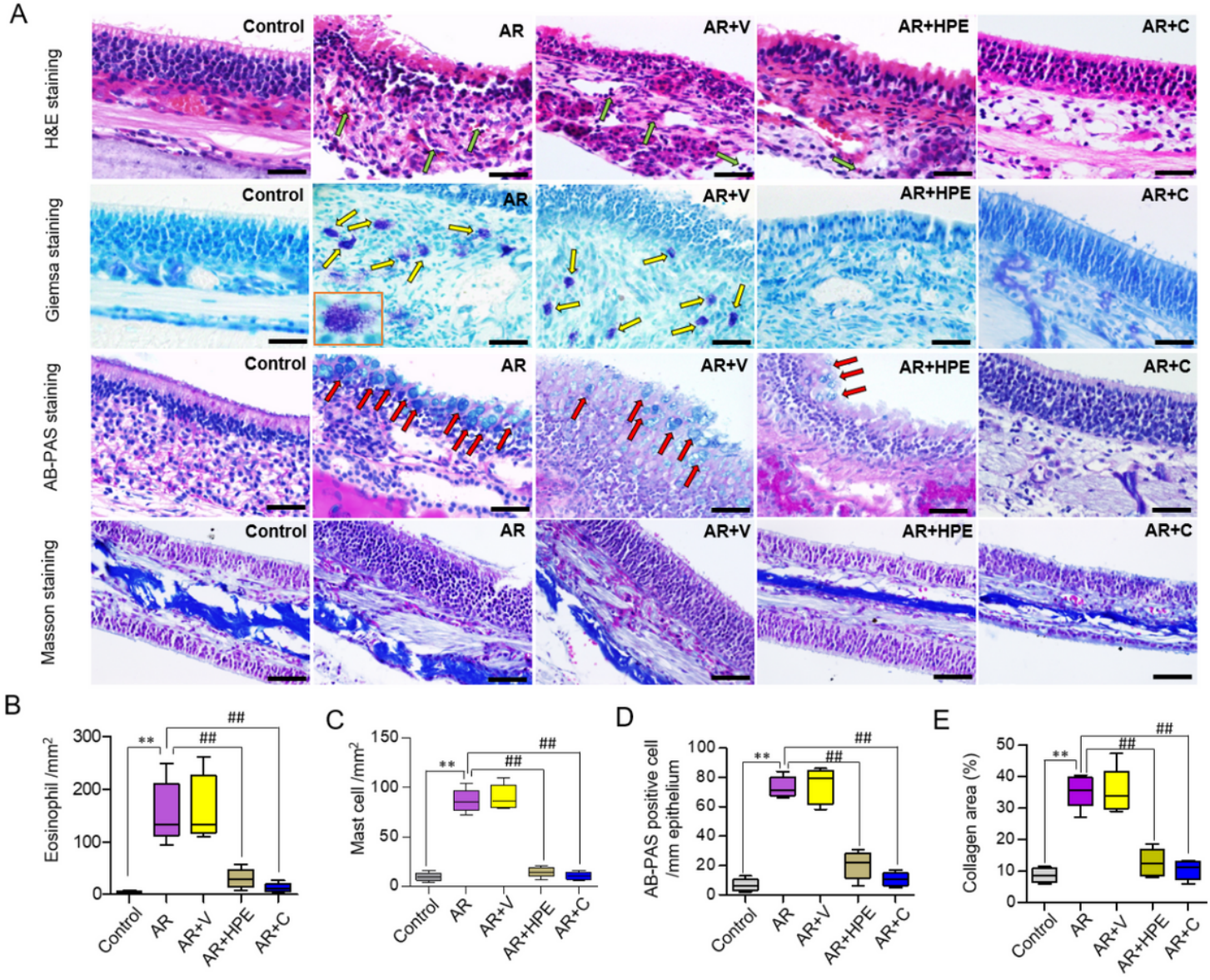

Figure 2

Effects of HPE on the histological changes of the nasal mucosa in AR rats. (A) Histopathological changes in the nasal mucosa of rats as detected by H&E (green arrows, eosinophils), Giemsa (yellow arrows, mast cells), AB-PAS (red arrows, goblet cells) and Masson staining (n=5, scale bar = 50μm). Statistical analysis for (B) eosinophils, (C) mast cells (D) goblet cells and (E) extracellular matrix in the nasal mucosa. The numbers of eosinophils and goblet cells were counted under a microscope at x400 magnification. Values are expressed as means ± SEM. $^{**}p < 0.01$ vs. Control group; $^{\#\#}p < 0.01$ vs. AR group. AR: allergic rhinitis; V: vehicle; HPE: human placenta extract; C: cetirizine; H&E: hematoxylin and eosin; AB-PAS: alcian blue and periodic acid-schiff.

Fig.3

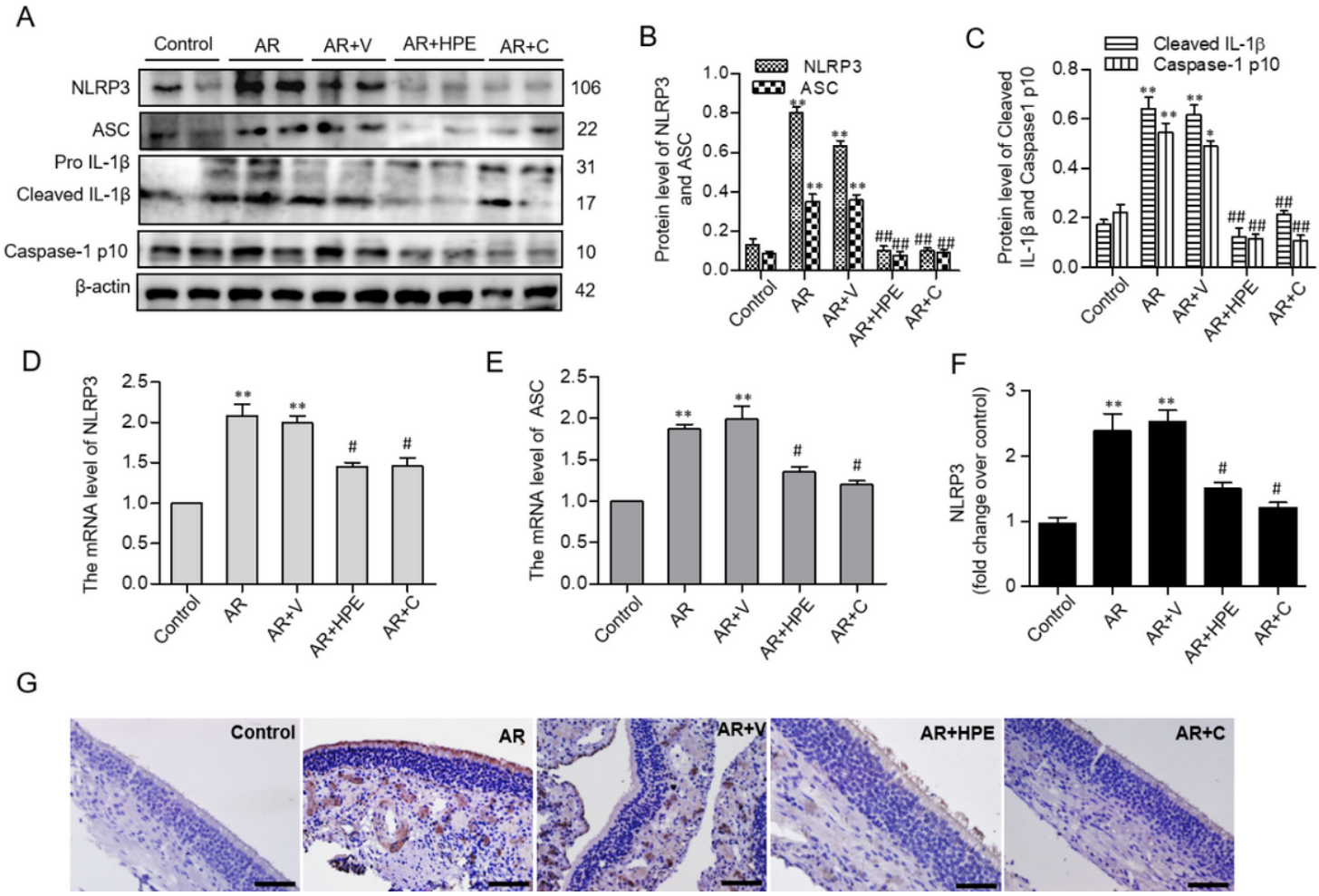

Figure 3

Effects of HPE on the NLRP3 inflammasome activation in AR rats. (A) The protein levels of NLRP3, ASC, cleaved IL-1β and caspase-1 p10 were detected by western blots in nasal mucosa of AR rats. (B-C) Quantitative analysis of the NLRP3, ASC, cleaved IL-1β and caspase-1 p10 from the Western blot data (n=5). (D-E) The mRNA levels of NLRP3 and ASC were detected by RT-qPCR (n=5). (F) The quantification of NLRP3 expression in rat nasal mucosa detected by immunohistochemical staining. (G) Representative pictures of NLRP3 immunohistochemical staining in rats (n=5, original magnification, x400, scale bar = 50μm). Values are expressed as means ± SEM. $^{*}p < 0.05$, $^{**}p < 0.01$ vs. Control group; $^{\#}p < 0.05$, $^{\#\#}p < 0.01$ vs. AR group. AR: allergic rhinitis; V: vehicle; HPE: human placenta extract; C: cetirizine.

Fig.4

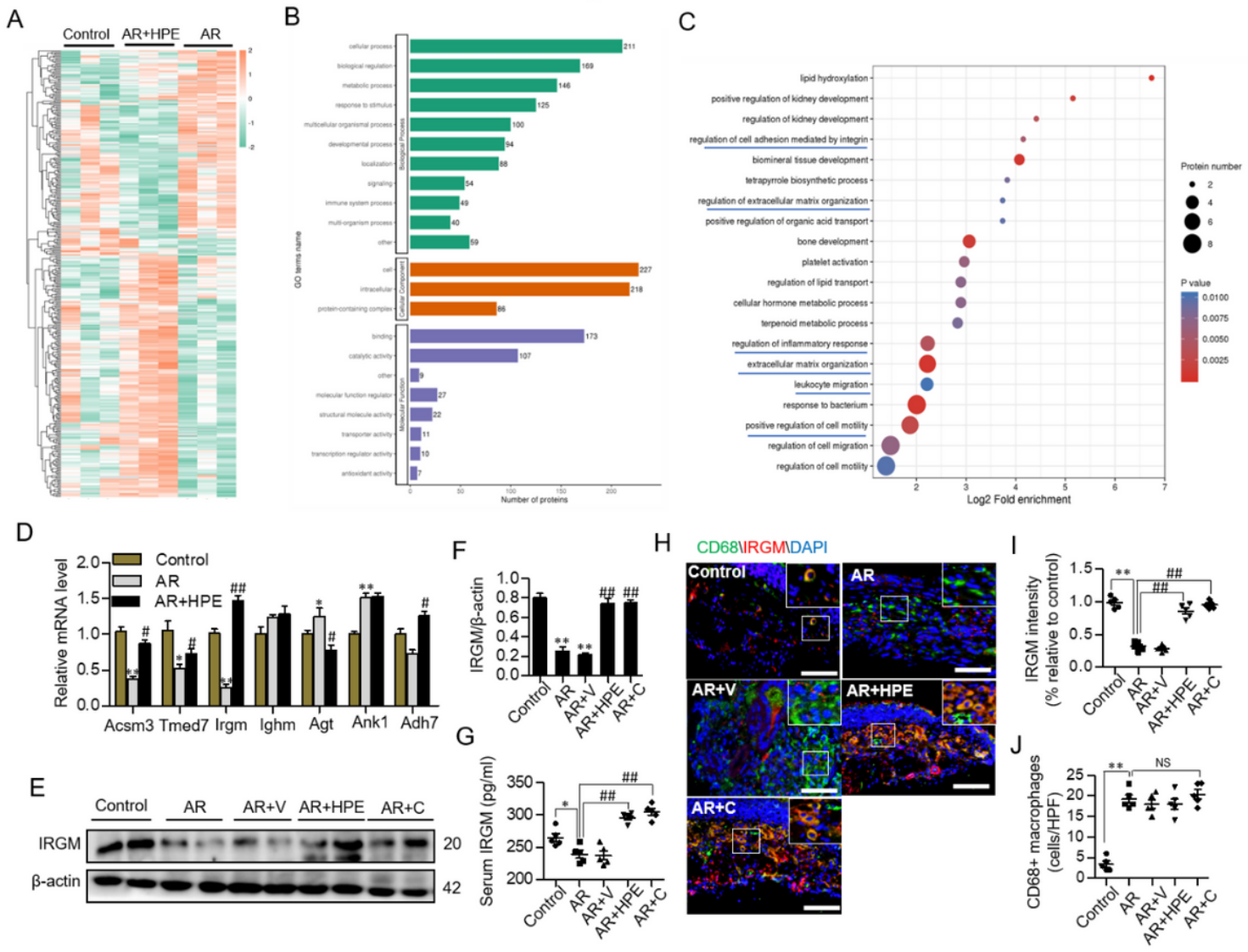

Figure 4

Effects of HPE on the expression of IRGM in AR rats. (A) Hierarchical clustering of the differentially expressed genes identified by high-resolution LC-MS/MS analysis. (B-C) Gene ontology (GO) and Kyoto Encyclopedia of Genes and Genomes (KEGG) pathway analysis for classification of the differentially expressed genes based on the proteomics. (D) 7 differentially expressed factors with significant changes in HPE-treated group were verified by qRT-PCR (n=5). (E-F) The protein level of IRGM was detected by western blots in nasal mucosa of AR rats (n=5). (G) The contents of IRGM in the serum of AR rats were measured using ELISA (n=5). (H) The colocation of IRGM and CD68 was detected by double immunofluorescence staining (n=5, original magnification, x400, scale bar = 50μm). (I) Statistical analysis for IRGM expression. (J) The number of macrophages infiltrating in the nasal mucosa. The number of macrophages were counted under a microscope at x400 magnification. Values are expressed as means ± SEM. $^{*}p<0.05$, $^{**}p< 0.01$ vs. Control group; $^{\#}p<0.05$ $^{\#\#}p< 0.01$ vs. AR group. AR: allergic rhinitis; V: vehicle; HPE: human placenta extract; C: cetirizine.

Fig.5

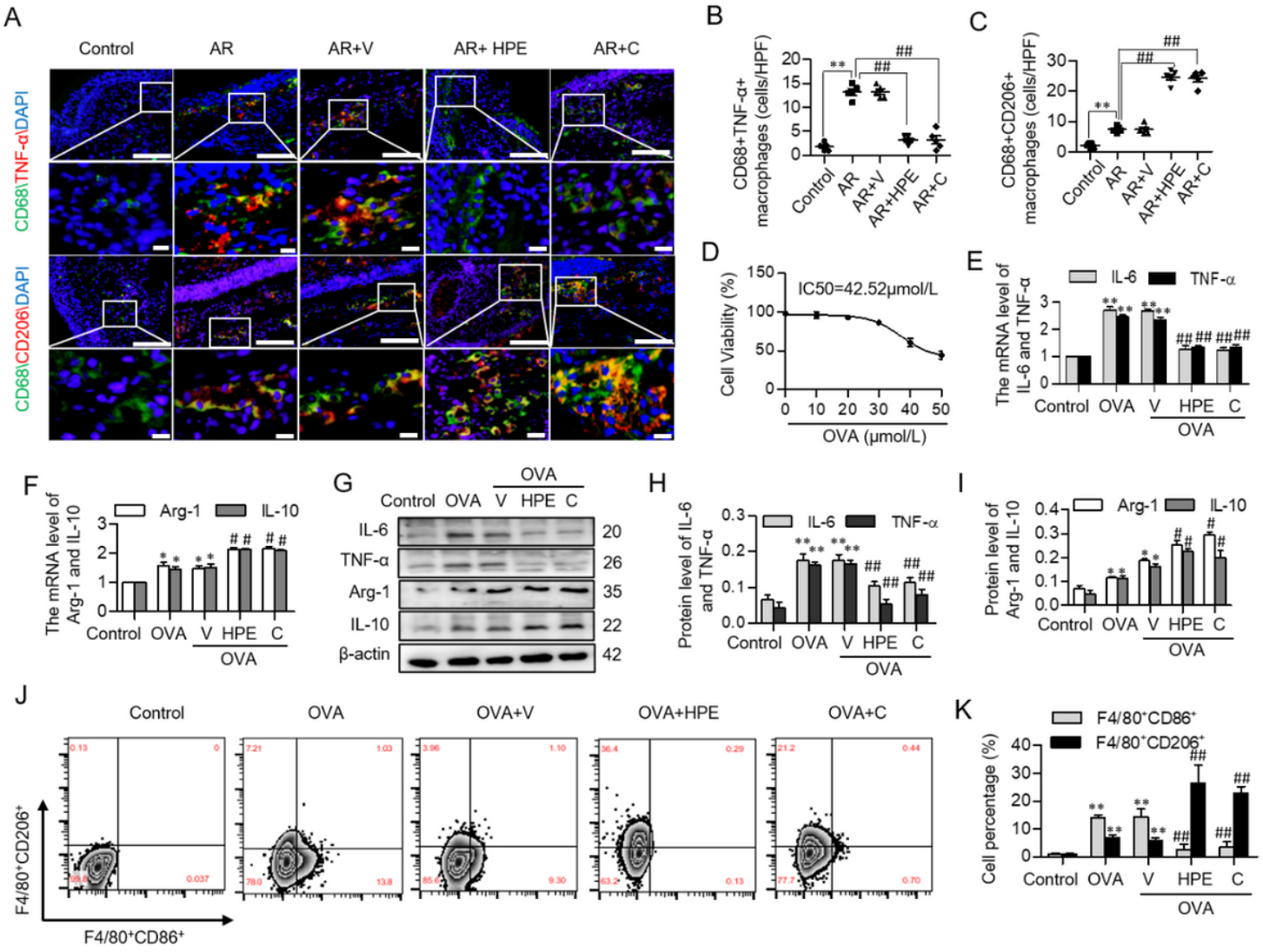

Figure 5

HPE regulates macrophage polarization in AR rats and MH-S cells. (A) The M1 and M2 polarization was detected by double immunofluorescence staining. (n=5, original magnification, x400, scale bar = 50μm or 20μm). Statistical analysis for the number of (B) M1 macrophages and (C) M2 macrophages infiltration in the nasal mucosa. The number of macrophages were counted under a microscope at x400 magnification. Values are expressed as means ± SEM. $^{**}p < 0.01$ vs. Control group; $^{\#\#}p < 0.01$ vs. AR group. (D) Cell viability was assessed with Cell Counting Kit-8 (CCK-8). (E- F) The mRNA levels of IL-6, TNF-α, Arg-1 and IL-10 were detected by RT-qPCR (n=5). Values are expressed as means ± SEM. $^{*}p < 0.05$, $^{**}p < 0.01$ vs. Control group; $^{\#}p < 0.05$, $^{\#\#}p < 0.01$ vs. OVA group. (G) The protein levels of IL-6, TNF-α, Arg-1 and IL-10 were detected by western blots in OVA-stimulated MH-S cells. (H-I) Quantitative analysis of the IL-6, TNF-α, Arg-1 and IL-10 from the Western blot data (n=5). Values are expressed as means ± SEM. $^{*}p < 0.05$, $^{**}p < 0.01$ vs. Control group; $^{\#}p < 0.05$, $^{\#\#}p < 0.01$ vs. OVA group. (J-K) Representative flow cytometry results (J) and summarized percentages (K) of $CD86^{+}$ and $CD206^{+}$ cells in the $F4/80^{+}$ macrophages

(n=3). Values are expressed as means ± SEM. $^{**}p < 0.01$ vs. Control group; $^{\#\#}p<0.01$ vs. OVA group. AR: allergic rhinitis; V: vehicle; HPE: human placenta extract; C: cetirizine; OVA: ovalbumin.

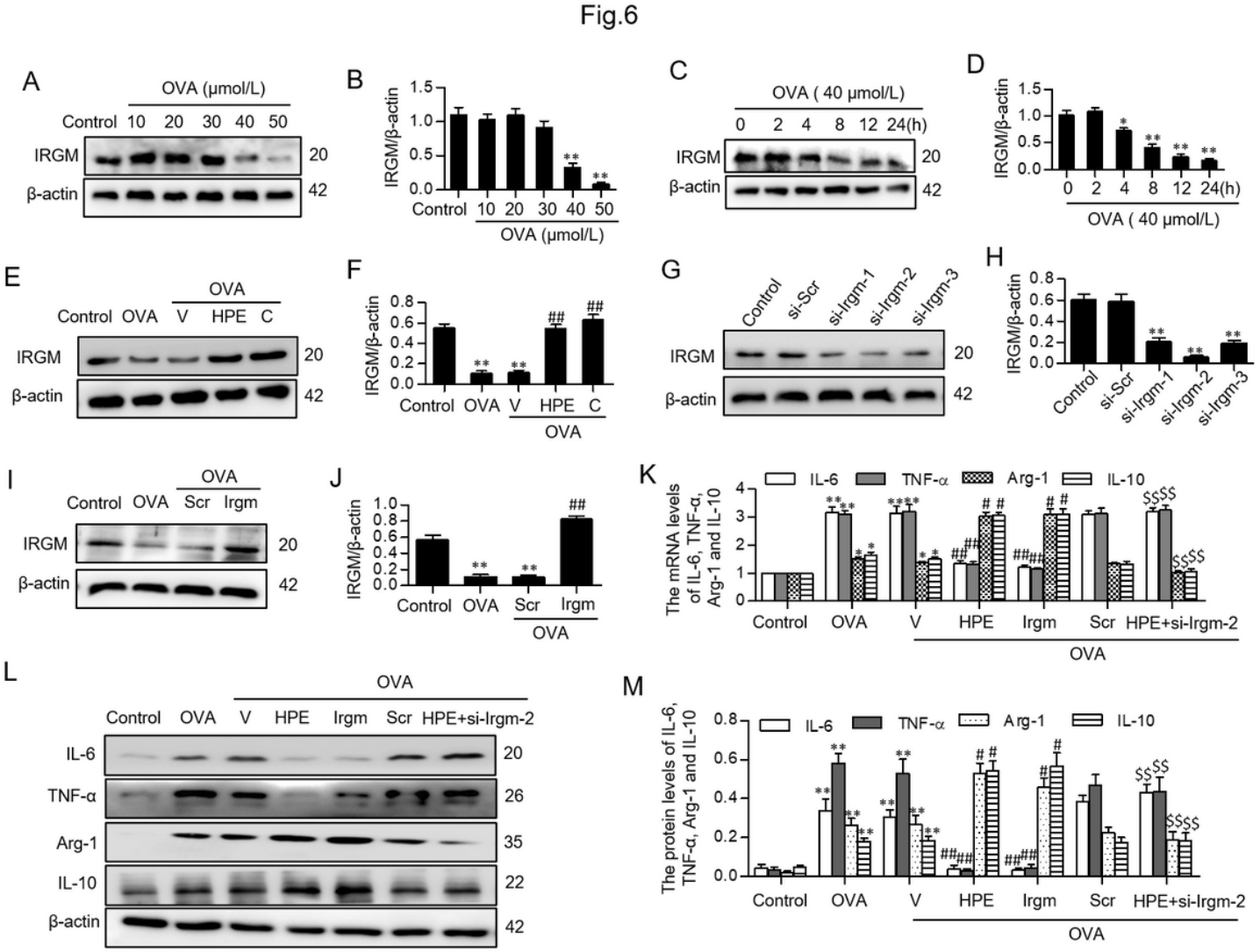

Figure 6

HPE regulates OVA-induced polarization of MH-S cells by upregulating IRGM. MH-S cells were serum starved for 24 h and cultured with different concentrations of OVA (0–50μM) for 24 h. (A-B) Dose–dependent effects of OVA on IRGM protein were evaluated by western blot (n = 6). Values are expressed as means ± SEM. $^{**}p < 0.01$ vs. Control group. (C-D) MH-S cells were serum starved for 24 h and cultured with OVA (40μM) at various time points. Time course-response of OVA (40μM) on IRGM protein expression were evaluated by western blot (n = 6). Values are expressed as means ± SEM. $^{*}p < 0.05$, $^{**}p < 0.01$ vs. 0h. (E-F) The protein level of IRGM was detected by western blots in OVA-stimulated MH-S cells (n=6). Values are expressed as means ± SEM. $^{**}p < 0.01$ vs. Control group; $^{\#\#}p< 0.01$ vs. OVA group. (G-H) The representative Western blot and quantification analyses of IRGM in MH-S cells transfected with IRGM siRNA. $^{**}p < 0.01$ vs. Control group. (I-J) The efficacy of IRGM overexpression plasmid was verified by western blot (n=6). $^{**}p < 0.01$ vs. Control group; $^{\#\#}p< 0.01$ vs. OVA group. (K) The mRNA levels of IL-6,

TNF-α, Arg-1 and IL-10 were detected by RT-qPCR (n=6). (L-M) The representative Western blot and quantification analyses of IL-6, TNF-α, Arg-1 and IL-10 in MH-S cells (n=6). Values are expressed as means ± SEM. $^{*}p < 0.05$, $^{**}p < 0.01$ vs. Control group; $^{\#}p < 0.05$, $^{\#\#}p < 0.01$ vs. OVA group; $^{\$\$}p < 0.01$ vs. HPE group. Scr: scramble; V: vehicle; HPE: human placenta extract; C: cetirizine; OVA: ovalbumin.

Fig.7

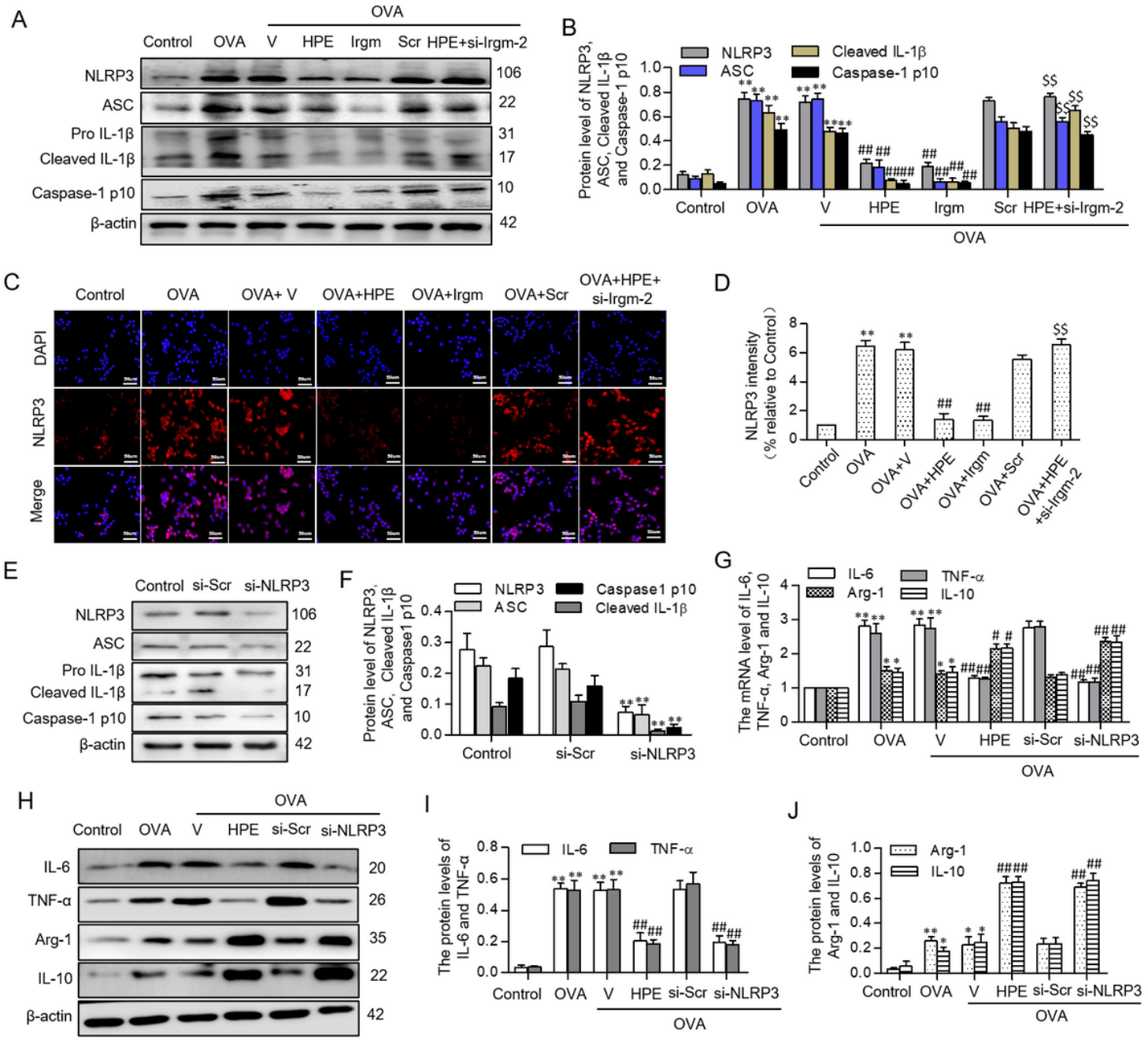

Figure 7

IRGM regulates MH-S cells polarization via suppressing NLRP3 inflammasome. (A-B) The representative Western blot and quantification analyses of NLRP3, ASC, Cleaved IL-1β and Caspase1 p10 in MH-S cells (n=6). Values are expressed as means ± SEM. $^{**}p < 0.01$ vs. Control group; $^{\#\#}p < 0.01$ vs. OVA group; $^{\$\$}p <$

0.01 vs. HPE group. (C-D) The expression levels of NLRP3 were analyzed by immunofluorescence in MH-S cells (n=6, original magnification, x400, scale bar = 50μm). Values are expressed as means ± SEM. $^{**}p <$ 0.01 vs. Control group; $^{\#\#}p <$ 0.01 vs. OVA group; $^{\$\$}p <$ 0.01 vs. HPE group. (E-F) The representative Western blot and quantification analyses of NLRP3, ASC, Cleaved IL-1β and Caspase1 p10 in MH-S cells transfected with NLRP3 siRNA (n=6). Values are expressed as means ± SEM. $^{**}p < 0.01$ vs. Control group. (G) The mRNA levels of IL-6, TNF-α, Arg-1 and IL-10 were detected by RT-qPCR (n=6). (H-J) The representative Western blot and quantification analyses of IL-6, TNF-α, Arg-1 and IL-10 in MH-S cells (n=6). Values are expressed as means ± SEM. $^{*}p < 0.05$, $^{**}p < 0.01$ vs. Control group; $^{\#}p < 0.05$, $^{\#\#}p <$ 0.01 vs. OVA group. Scr: scramble; V: vehicle; HPE: human placenta extract; C: cetirizine; OVA: ovalbumin.

Fig.8

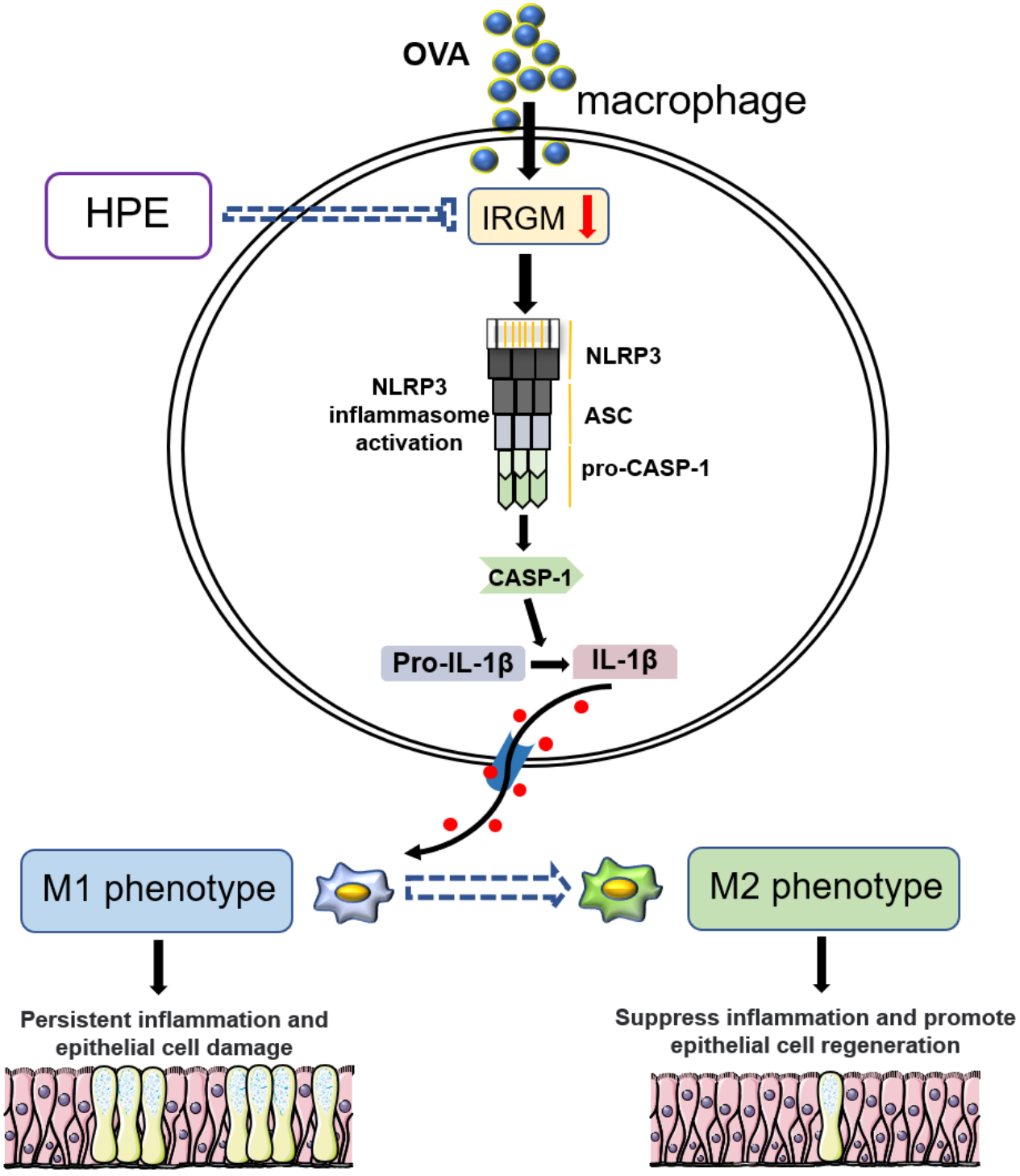

Figure 8

Schematic depiction of the protection role of HPE for AR. OVA leads to IRGM downregulation, resulting in macrophages M1 polarization through the activation of NLRP3 inflammasome. Macrophage M1 polarization further induces persistent inflammation and epithelial cell damage. HPE has protection for AR and the protection is achieved partly through suppressing M1 while promoting M2, the process which is mediated by IRGM via inhibiting NLRP3 inflammasome in AR.